Fundamental study of fluid transfer using electro-rheological effect

Yutaka Tanaka
Okayama University

Akio Gofuku
Okayama University

Fundamental Study of Fluid Transfer using Electro-Rheological Effect

Yutaka TANAKA* and Akio GOFUKU*

* Department of Systems Engineering, Okayama University,
3-1-1 Tsushima-Naka, Okayama, 700-8530, Japan

Abstract

Considering that there is no pump feeding an Electro-Rheological-Fluid, a new type of pump has been manufactured and fluid dynamic characteristics have been elucidated. This pump can feed the ERF by utilizing effectively the change in physical properties of the fluid by the application of voltage.

The principle and configuration of this pump and the methods of theoretical analysis are described, and the influence of the voltage on the feeding characteristics was examined. The dispersoidal ERF has been treated hitherto as a type of Newtonian fluid. However, experiments showed that not only the induced shear stress but also the viscosity is affected by the electric field strength and that the ERF must be treated as a pseudo-plastic flow. The method of analysis described here can be applied to design the pump differing in dimensions because the analysis gave qualitative evaluations about the flow rate and pressure difference.

1 Introduction

We showed in the previous reports[1, 2, 3] that the use of an Electro-Rheological-Fluid as a working fluid enables to control an artificial muscle and other pressure devices. However, the ordinary pump-valve system clogs with the particles contained in the ERF and becomes useless at once. Hence, we checked whether there are some pumping systems that can feed ERFs or not in JICST and literature, and found that there is no appropriate pump and research. The use of gear pumps for high viscous fluids is considered but these pumps are not effective because ERF is damaged owing to the smash of particles. The concept of pumping effect using an ion drag force is seen in the reference[4] but the method proposed in this report is based on the different concept.

The previous reports assumed that the flow was of the Newtonian having the constant viscosity irrespective of the change in flow rate and pressure. Thereafter we have carried out many experiments for wide flow and pressure regions and for the flow fields where a pipe flow and a peripheral flow are combined together, and have had the doubt about the constancy of viscosity. The second object is to obtain the answer to this doubt and to examine the effects of the electric field E on the induced shear stress τ_E and the viscosity μ_E. In this paper we exhibit that ERF flow field should be treated as a pseudo-plastic (Non-Bingham) one, and we elucidate the difference between the Newtonian and the Non-Bingham flow field.

This report proposes an ERF feeding method and examines theoretically and experimentally how ERF feeding is achieved, where use is effectively made of the electric characteristic that the apparent viscosity of ERF is controlled by the high voltage application. The functions, abilities and characteristics of this pump are evaluated and its practicality is judged. Firstly the princple and structure of this pump and the method of analysis are described. Next the influences of voltage applied and revolution speed on the feeding characteristics are examined. Also the influences of voltage on the induced shear stress and the viscosity are examined.

2. ERF feeding pump

Figure 1 illustrates the configuration of the pump that feeds ERF. This pump utilizes the principle where the ERF is fed by the increase in the viscosity when a high voltage is applied on a pair of electrode disks through a

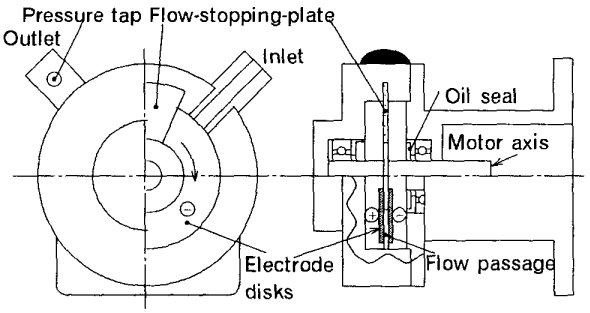

Fig.1 Schematic representation of an ERF－pump

bearing and ERF is filled in the passage between them.

The ERF pump is driven by a motor and the ERF is fed into the narrow passage interposed by a pair of opposed rotating electrode disks. Due to the shear stress induced by the voltage applied to the disks the ERF is fed to the outlet accompanied by the increases in pressure and flow velocity. As shown in this figure this pump has a simple passage structure and any types of vanes such as employed in the ordinary pump are unemployed. Only a flow stopping plate exists that divides the inlet and the outlet.

Figure 2 shows the constitution of the experimental apparatus. As pump dimensions the inner and outer diameter $2b$, $2a$ are respectively 4cm and 8cm, and the space h between rotating disks is 2mm, the sector angle of the flow stopping plate is 40° ($=0.22\pi$), and the plate thickness is 1.8mm. The parts needed electric conductivity are made of brass and the other parts are made of vinyl chloride resin or engineering plastics. The pump axis is driven by an induction motor and a speed reduction device. As an ERF the standard sample SR-1 (mean particle diameter 3.5μ) of Japan Rheology Society was used.

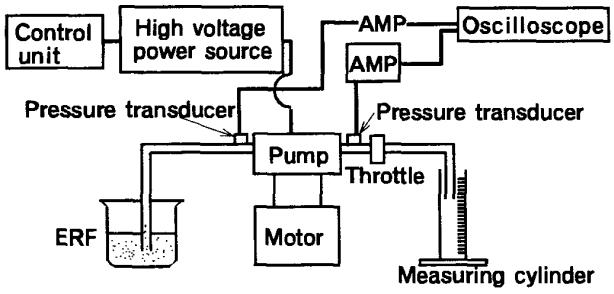

Fig. 2 Confiuration of the experimental setup

3 Theory

Steady flow field is assumed and the following assumptions are postulated:

(1) The flow fields in the inlet and outlet pipes and in the pump are laminar ones. It is assumed that the ERF behaves as a non-Bingham (Pseudo-plastic) fluid.

(2) The viscosity is changed with the changes in the electric field E and the velocity gradient ($G \equiv |\partial u/\partial r|$ in the pipe and $G \equiv |\partial u/\partial y|$ in the pump).

(3) The fluid that enters into the pump from the inlet flows only along the circumferential direction-θ and flows out from the outlet.

(4) The influences by the radial pressure distributions in the pump are disregarded and the pressure gradient is caused only in θ-direction.

(5) Because of the dragging effect of the fluid by the walls the laminar flow field is formed in the central region of the pump passage, where there are a plug flow region having flat velocity distribution and the region where the flow velocity increases in y-direction toward the peripheral wall surfaces. However, the flow distribution in the passage without voltage application becomes the laminar one.

Referring the measured values for $E = 0$ obtained by the company that proposed ERF, the viscosity μ is expressed as

$$\mu = \mu_E (G/G_0)^m \quad \cdots\cdots\cdots\cdots (1)$$

Where, μ_E becomes μ_0 at zero electric filed application $E = 0$ and the velocity gradient of $G=G_0$. The viscosity μ_E for dispersoidal ERF has been treated as constant against the change in electric field strength[5], and the feasibility of the treatment like this is confirmed experimentally in this report. The exponent m of the velocity gradient is zero for the Newtonian fluid; however, m was between -1/4 and -1/2 from the measurement of ERF. Based on the experimental result shown in the following Fig. 3 the analysis is made on the assumption that the exponent m is -1/2.

3.1 The flow in the inlet and outlet pipes and the estimation of pressure loss

Referring the viscosity given by Eq. (1), the relation between the flow rate Q in the inlet and outlet pipes and the pressure loss $P = -\partial p/\partial x$ is derived. Here, x denotes the distance along pipe axis and p the pressure. If r refers to radial distance, u the flow velocity, $\tau = -\mu \cdot \partial u/\partial r$ the shear stress, then we have

$$1/r \cdot \partial (r \tau)/\partial r = P \quad \cdots\cdots\cdots\cdots (2)$$

Considering that the viscosity is expressed as Eq. (1), Eq. (2) is integrated under the boundary condition that $\partial u/\partial r = 0$ along the central axis $r = 0$ and $u = 0$ on the pipe wall $r = R$, and we have

$$u = P^2 (R^3 - r^3)/(12 \mu_e^2 G_0) \quad \cdots\cdots\cdots\cdots (3)$$

From the integration of the above equation, the relation between the flow rate Q and the pressure loss P becomes

$$Q = \pi P^2 R^5/(20\mu_c^2 G_0) \quad \cdots\cdots\cdots (4)$$

Considering that several pipes differing in length dx and radius R are joined together, the following integral expression is obtained

$$\Delta p = -\sqrt{20\mu_c^2 G_0 Q/\pi} \int (1/R^{2.5})\,dx \quad (5)$$

Namely we can derive the result that the pressure loss is proportional to the square root of the flow rate and is inversely proportional to the 2.5-th power of the pipe inner radius R. Note that this equation differs much compared to the well-known relationship for Newtonian flow $Q = \pi PR^4/(8\mu)$ obtained under the assumption that the viscosity is constant[7], where the pressure loss is proportional to the flow rate and is inversely proportional to the 4-th power of R.

From Eq. (3) the velocity gradient $G=5Q/(\pi R^3)$ is derived. Since the shear stress $\tau_w = 5\mu_w Q/(\pi R^3)$ acting on the pipe peripheral surface balances with the pressure gradient P, the viscosity on the wall μ_w is evaluated from the following equation if P and Q are measured.

$$\mu_w = \pi PR^4/(10Q) \quad \cdots\cdots\cdots (6)$$

In Fig. 3 the viscosity data and the plots + measured by an ERF manufacturing company by the use of a coaxial rotating cylinder viscometer are arranged against the velocity gradient G. Here, our data are obtained by substituting the flow rate and pressure gradient for different radius pipes into Eq. 6). The solid line represents the experimental equation(1), and the measured data mean that the viscosity of ERF varies greatly with the velocity gradient. It is apparent from this figure that the viscosity cannot be treated as constant irrespective of the changes in velocity gradient as has been carried out ordinally in the previous analyses.

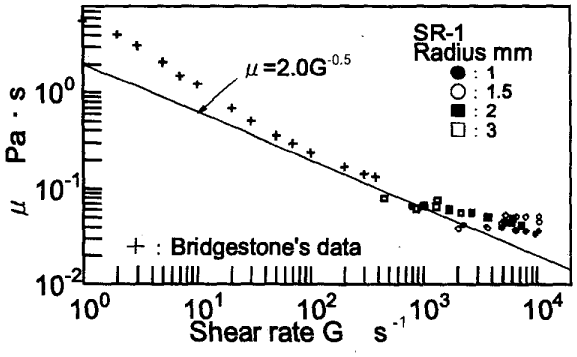

Fig.3 Relationship between shear rate and viscosity

Figure 4 represents the changes in velocity distribution and shear rate with non-dimensional pipe radius r/R for Newtonian and Non-Bingham fluid. The ratio u/u_{mean} indicates the flow velocity profile normalized by the average velocity in a pipe $u_{mean}=Q/(\pi R^2)$, and exhibits that the Newtonian fluid has the form of a paraboloid of revolution but the profile of Non-Bingam fluid is being flattened compared to the one of Newtonian fluid. The shear ratio G/Gw is non -dimensionalized against the shear rate Gw at wall surface. As being apparent from the integration of Eq. (2), the shear stresses for both fluids increase linearly from zero at pipe center to the maximum at wall; therefore, it is observed that the shear rate G/Gw for Newtonian fluid also increases linearly toward the wall but G/Gw for Non-Bingham fluid increases gradually.

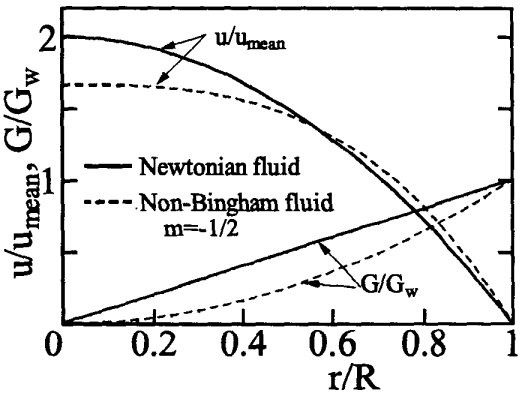

Fig. 4 Comparison between the radial flow profiles in a pipe without electric application for Newtonial fluid and Non-Bingham fluid

3.2 Analysis of the flow in the pump

Figure 5 shows the analyzing model of the flow in this pump. The circumferential distance is denoted as $x=r\theta$, the flow velocity in the direction $x(\theta)$ as u, depth distance as y. The flow in the radial direction r and the pressure difference caused by the kinematic energy are small enough and are neglected. The relation between the pressure change and the shear stress τ in the region $y \geqq 0$ namely $\partial u/\partial y \geqq 0$ is expressed by using the shear stress $\tau_E(E)$ induced by the electric field strength E as follows

$$\partial p/\partial x + \partial \tau/\partial y = 0 \qquad \cdots\cdots\cdots (7)$$

$$\tau = -\mu \cdot \partial u/\partial y - \tau_E(E) \qquad \cdots\cdots\cdots (8)$$

The boundary conditions give

$$\left.\begin{array}{l} \partial u/\partial y = 0 \text{ in } y \leqq \lambda \\ \quad \text{within the plug flow position } \lambda, \\ u = U(r) = r\omega \text{ at } y = h/2 \\ \quad \text{on the wall surface} \end{array}\right\} \cdots\cdots\cdots (9)$$

where ω refers the angular velocity of the rotation pump and peripheral wall, $U(r)=r\omega$ the peripheral wall speed, h the passage width between the electrodes. The solid line and the dashed line in the upper part in Fig. 5 respectively represent the velocity profiles with and without the electric field. Taking Eq. (1) into consideration, putting $m=1/2$, $A=1/(3\mu_E^2 G_0)$, and solving Eqs. (7, 8, 9), then we have the velocity u between $h/2 \geqq y \geqq \lambda$

$$u = A(\partial p/\partial \theta)^2[(y-\lambda)^3 - (h/2-\lambda)^3]/r^2 + r\omega \qquad (10)$$

the minimum velocity u_{min} in $y \leqq \lambda$

$$u = u_{min} = -A(\partial p/\partial \theta)^2 (h/2-\lambda)^3/r^2 + r\omega \qquad (11)$$

The plug flow position λ is estimated as the axial position y where the shear stress becomes equal to the induced one $\tau_E(E)$ in consideration of the fact that the shear stress is increasing in proportion to y up to the stress

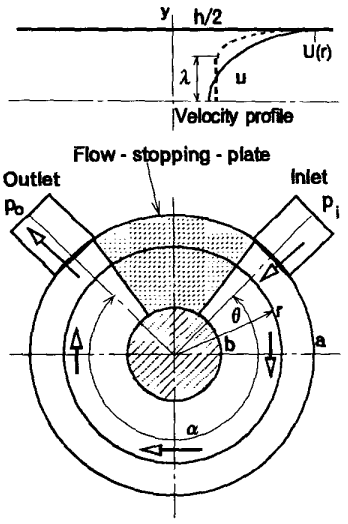

Fig.5 Analytical model of the flow in an ERF–pump

τ_w at the wall surface[7], and is expressed as

$$\lambda = \tau_E(E)/[\partial p/\partial x]_E \qquad \cdots\cdots\cdots (12)$$

or $\lambda = rS$, $S = \tau_E(E)/(\partial p/\partial \theta)_E$ (13)

Integration of Eqs. (10, 11) within the passage width from $y=0$ to $y=h/2$ and the radius from $r=b$ to $r=a$ gives

$$Q = \omega h(a^2-b^2)/2 - (3/2)A(\partial p/\partial \theta)^2 (h/2)^4 (1/b - 1/a) + (1/6)A(\partial p/\partial \theta)^2 \{S^4(a^3-b^3) - 18(h/2)^2 S^2(a-b) + 24(h/2)^3 S[\ln(a) - \ln(b)]\} \qquad \cdots\cdots\cdots (14)$$

The first term of RHS in Eq. (14) represents the rotation volume and its ratio against Q expresses volume efficiency. In the passage without electric field application only the first and second terms of RHS are meaningful.

3.3 Calculation methods of flow rate Q, and pressures p_o and p_i

In the experiment the ERF is sucked through a pipe of inner radius R_1 and length L_1 from the vessel opened to atmospheric pressure p_a as shown in Fig. 2 and it is discharged through a pipe of inner radius R_2 and length L_2 into a measuring vessel. Then the flow rate Q, suction pressure p_i and discharge pressure p_o are measured when the electric field E is applied on the rotating electrode disks via a bearing. From Eq. (5) the square of the pressure summation Δp between the pressure losses $p_a - p_i$ in the suction pipe and the loss $p_o - p_a$ in the discharge pipe becomes

$$(\Delta p)^2 = 20\mu_c^2 G_0/\pi \left(L_1/R_1^{2.5} + L_2/R_2^{2.5}\right)^2 Q \qquad (15)$$

The measured flow rate and the square of pressure loss are plotted in Fig. 6. The relation between them is fitted well to the linear line which passes through the origin although the data under various electric fields E and rotation velocity ω are plotted. If the coefficient of the RHS Q of Eq. (15) is denoted as K, then the value obtained by the least square method becomes $K = 20\mu_c^2 G_0/\pi \left(L_1/R_1^{2.5} + L_2/R_2^{2.5}\right)^2 = 6.56 \times 10^{13}$ [Pa^{2}s/m^3], and this value agrees well with the value evaluated when the pipe dimensions L_1 and R_1 are substituted into this equation. Small dispersions in the plots are considered as being due to the influences of temperature on μ_c because the data were obtained in different days and hours. However, the fact that the relationship is arranged into one linear line means that the viscosity can be represented by Eq. (1) and the fluid should be treated as the pseudo plastic fluid.

The pressure loss Δp equals the pressure increase (head) in the pump given by Eq. (14). The flow rate Q and the pressure Δp are evaluated by solving simultaneously this equation and the shear stress $\tau_E(E)$ equation, and inversely, the shear stress and viscosity can be known by substituting the measured values E, Q, and Δp into these equations.

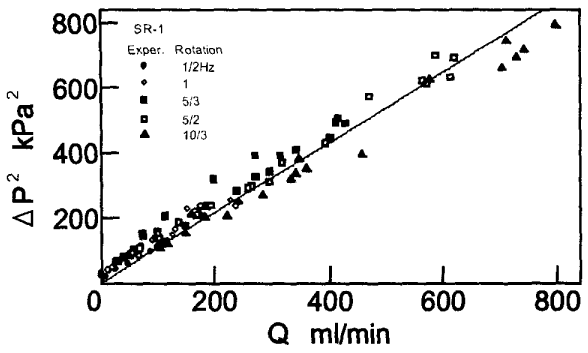

Fig.6 Relationship between the flow rate and the square of pressure increase

4 Results and considerations

Although long computation procedures are needed the viscosity μ_E and the shear stress τ_E under the identical electric field strength E are estimated by substituting a pair of the measured flow rate Q and the pressure increase Δp into the flow rate equation (14). Where use is made of the coefficient $A=1/(3\mu_E^2 G_0)$.

Figures 7 and 8 depict respectively the variations of the viscosity μ_E and the shear stress τ_E with the change in the electric field strength E. This ERF is the dispersoidal one and the effect of E on the viscosity is disregarded because the measurement is difficult. However, it is apparent from Fig. 7 that the viscosity cannot be regarded as being constant with the electric field change. The bridge structure of the dispersed particles is generated in the flow field with an electric field application, and this phenomenon makes rise in the particle density and will increase the fluid viscosity. In order to express appropriately the experimental result this report regards that also the viscosity μ_E changes with increasing E in the following equation (16). Taking into consideration of the fact that the pressure loss is governed by the large velocity gradient G at the pipe wall and the variations of measured results shown in Fig. 3 the viscosity is regarded as being expressed in the empirical Eq. (16) in such a way that the equation fits well the data in the range $G>10s^{-1}$ and it passes through the point $\mu_0=2$ Pas at $G_0=1s^{-1}$. The coefficient C_μ is then taken as 1.7.

$$\mu_E=\mu_0\sqrt{1+C_\mu E} \qquad \cdots\cdots\cdots (16)$$

The dashed curve and the dotted curve in Fig. 8 exhibit respectively the average shear stresses τ_E for the pump flow and the annular pipe flow obtained by regarding that the viscosity is held constant as μ_0. The other data represent τ_E that are derived with the viscosity and are estimated in consideration of the influence of the electric field. The plots $\times$ are the measured data for the flow in the annular pipes of o. d. 3mm and i. d. 0. 5mm and the other plots are the data for the pump. Seeing these results it is found that (1) the shear stress τ_E obtained by regarding that the viscosity is also affected by the electric field becomes about a half of the value obtained by regarding that the viscosity is kept constant, (2) the shear stress in the annular pipe tends to increase in proportion to the square of the electric field but the shear stress in the pump tends to saturate in the region where E is greater than 1kV/mm.

The saturated shear stresses in the range where E is greater than 1kV/mm are dispersed with the changes in the rotation velocity; however, the following analysis is carried out by regarding that this is represented by Eq. (17) as shown by the solid line in the figure,

$$\left.\begin{aligned}\tau_E &= 50\,E^2 \quad \text{for} \quad E\leqq 1\text{kV/mm}\\ \tau_E &= 50 \quad\;\; \text{for} \quad E>1\text{kV/mm}\end{aligned}\right\} \qquad (17)$$

4.1 Comparison of the experimental results with the calculation ones

In this section the experimental results of Q and Δp are shown and these are compared with the theoretical ones,

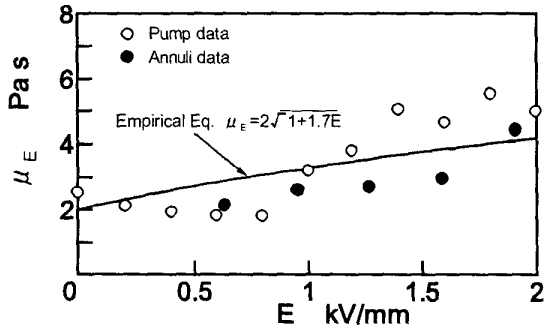

Fig.7 Dependence of viscosity on the electric field strength

and the validity of the theory is examined. In this examination, theoretical results are derived by using the empirical equations (16, 17) for the physical properties such as viscosity and shear stress of ERF and the relation (16) between the pressure losses and the flow rate.

Figures 9 shows the changes in the flow rate Q and pressure increase Δp with the electric field. It is seen that the flow rate and the pressure increase with an increase in electric field strength, and that the calculated results agree nearly quantitatively with the measured results. When the rotation velocity ω is changed, the flow rate increases almost linearly as inferred from Eq. (14) even if there is a decrease in viscosity as shown in Fig. 3 and the pressure increases in proportion to the square root of ω.

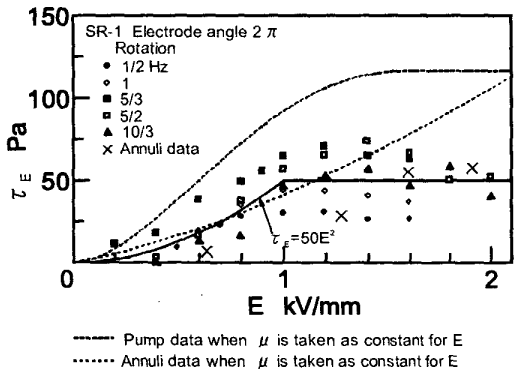

Fig.8 Dependence of induced shear stress τ_E on the electric field strength

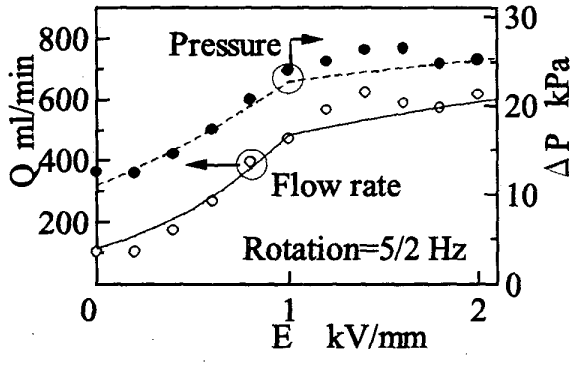

Fig. 9 Influence of electric field strength on the increases in flow rate and pressure

At present, the rotation speed cannot be elevated to the desired speed because of the flexibility of the non-metal and handmade device; however, we hope that this device can supply the ERF fluid at the pressurized level more than ten times the present level.

5 Concluding remarks

In consideration of the fact that there is no pump for supplying the ERF a new type of pump was devised, which can feed the ERF containing dispersoidal particles. The relationship between the pressure head and the flow rate was studied and the effects of the electric field on the viscosity and the shear stress were examined. Summarizing the results obtained the following conclusions are drawn.

(1) Although there are some points to improve the present pumping method generates large flow rate and pressure increase by applying the electric field and is effective as the method for feeding the ERF.

(2) The present method of analysis can evaluate the pressure increase and flow rate generated by the fluid transfer.

(3) Even in the use of the dispersoidal ERF not only the shear stress but also the viscosity should be treated as the ones for the pseudo plastic fluid in order to express correctly the flow field.

References

[1] Tanaka, Y., Fundamental Study of Rubber Artificial Muscle, Trans. JSME-C, 58-54 (1992), 58-54.

[2] Tanaka, Y. and Gofuku, A, Development and Analysis of an ERF Pressure Control Valve, Mechatronics, 7-4 (1997), 317-335.

[3] Tanaka, Y. and Gofuku, Prediction Based on Electric-Fluid Method of Dynamic Responses of Pressurizing Devices Drived by Electro-Rheological Fluid, Trans. JSME-C, 64-621 (1998), 1743-1748.

[4] Kimura, Y., Report of ERF and its Application, P-SC221 (1994), 6-9, JSME.

[5] Furusho, J., Report of Control of Mechatronic Devices Using ERF, P-SC237(1996), 24, JSME.

[6] Schlichting, H., Boundary Layer Theory, 68-60 (1951), McGraw Hill.

[7] Ito, Fluid Dynamics for Scientist, 22 (1972), Maruzen.